Take a Look Back upon the Past Decade of Direct Torque Control

Isao Takahashi, *IEEE Fellow*, and Toshihiko Noguchi, *IEEE Member*

Department of Electrical and Electronic Systems Engineering,
Nagaoka University of Technology
1603-1 Kamitomioka, Nagaoka 940-21, Japan
Phone : +81-258-46-6000, Fax : +81-258-47-9500,
E-mail : taki@vos.nagaokaut.ac.jp, omom@vos.nagaokaut.ac.jp. WWW : http://pelab.nagaokaut.ac.jp

Abstract — **More than ten years have passed since direct torque control strategy of an induction motor was first reported. The strategy has featured direct control of a stator flux vector and an output torque instead of the conventional current control technique which has been employed in the field-oriented control, and has given a systematic solution to improve operating characteristics of not only the motor but also the PWM inverter. In the paper, looking back upon the fruitful past decade and looking at the present state of the strategy, several key techniques are reviewed. One of the techniques is improvement of the basic performance which was enabled by means of a double parallel PWM inverter, and it has made an ultimately quick torque response possible. Another technique is relevant to robust control, which makes the system insensitive to both stator and rotor resistance. Also, the latest technique which contributes to enhance further system performance is referred, which is a dither signal application to the direct torque control for acoustically silent drive.**

I. Introduction

DIRECT torque control of an induction motor was first reported about ten years ago, and it was inherently developed for the purpose of breaking through a common sense in those days, which was like that "There is nothing but field-oriented control to obtain a quick torque response by the induction motor" [1]. The direct torque control has been demonstrating its potential to optimize operating characteristics of the induction motor drive fed by a PWM inverter ever since [2]-[4]. As for the motor, the direct torque control has achieved as quick torque response as a dc motor, although the motor is not controlled by a conventional field-orientation method. Also, ripples of the stator flux and the output torque which are caused by PWM waveforms have been reduced effectively in the motor. On the other hand, from another viewpoint of the inverter, almost perfectly optimized PWM waveforms have been obtained owing to relay control of both the stator flux and the output torque by using an optimum switching table. The selection of the inverter output voltage vectors is performed so that the switching frequency of the inverter can be reduced and the optimized PWM waveforms can be generated. It is considered that there has never been such a concept to improve the various kinds of performance in the motor-inverter system at the same time.

In the paper, looking back upon the past decade and looking at the present state, several key techniques are reviewed, which have been adopted to the direct torque control to realize further improvement of the operating characteristics. Problems with regard to the improvement can be divided into two categories; one is enhancement of the basic control performance of the stator flux and the output torque [5]. The other is improvement of estimation technique of the stator flux and the output torque, which must be performed with less sensitivity to the motor parameters [6]. In what follows, not only solutions to those problems but also an up-to-date topic to make further improvement are described [7].

II. Improvement of Basic Performance by Double Parallel PWM Inverter

Fig. 1 shows a power circuit of a double parallel PWM inverter adopted to the direct torque control. Two voltage source inverters are commonly connected to a dc power source, while their outputs are connected to each other through inter-phase reactors. The inverter feeds an induction motor from center taps of the reactors. It is found that there are sixty-four

0-7803-3932-0

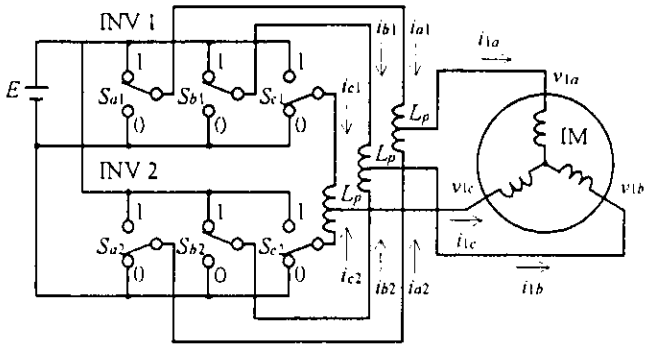

Fig. 1. Induction motor drive fed by double parallel PWM inverter.

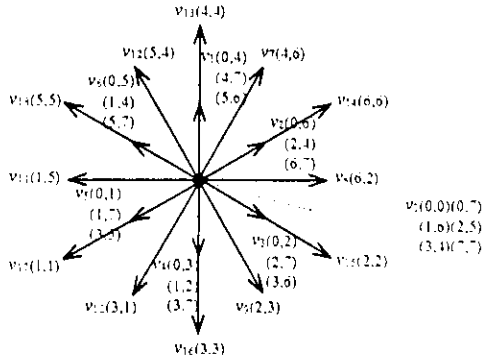

Fig. 2. Output voltage vectors of double parallel PWM inverter.

combinations of the inverter switching modes , whereas the number of possible output voltage vectors v_n is only nineteen as shown in Fig. 2.

In order to obtain a smooth locus of the stator flux vector ψ_1, it is necessary to divide a stationary plane for flux control, what is called $\alpha-\beta$ coordinates, into twelve sectors because the non-zero voltage vectors $v_1 \sim v_{18}$ have phase displacement of 30 degrees from each other. By alternating two of the $v_1 \sim v_{18}$, the ψ_1 can be controlled smoothly as illustrated in Fig. 3. On the other hand, the output torque T should be controlled as shown in Fig. 4 by applying the voltage vectors alternately to the motor as follows. When the output torque level is low, the zero and one of the non-zero voltage vectors are alternately output from the inverter to restrict the torque error within specified hysteresis band width. In this case, the non-zero vectors which have smaller amplitudes $v_1 \sim v_6$ are selected to rotate the ψ_1, and the zero vector v_0 is selected to stop the ψ_1. Once the output torque level becomes high enough, two kinds of non-zero voltage vectors $v_1 \sim v_6$ and $v_7 \sim v_{18}$ are alternately selected. In order to reduce the T gradually within the hysteresis band, one of the $v_1 \sim v_6$ is applied to the motor instead of v_0, which makes the ψ_1 rotate slowly.

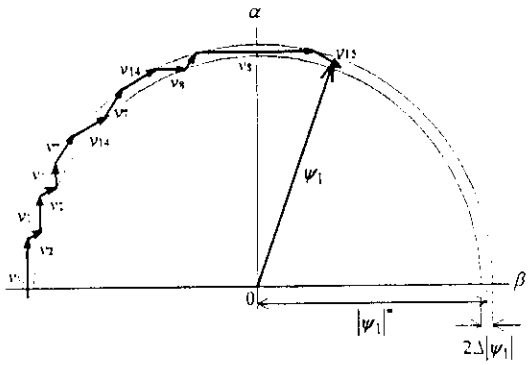

Fig. 3. Stator flux vector control.

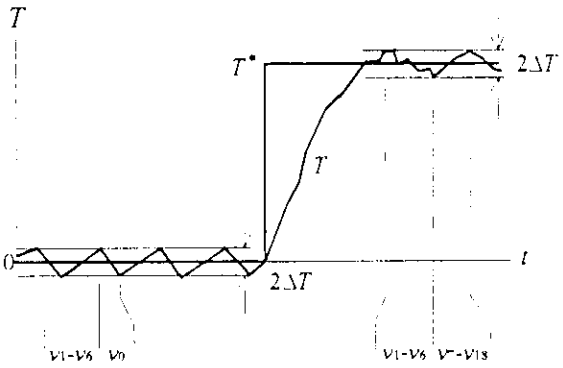

Fig. 4. Output torque control.

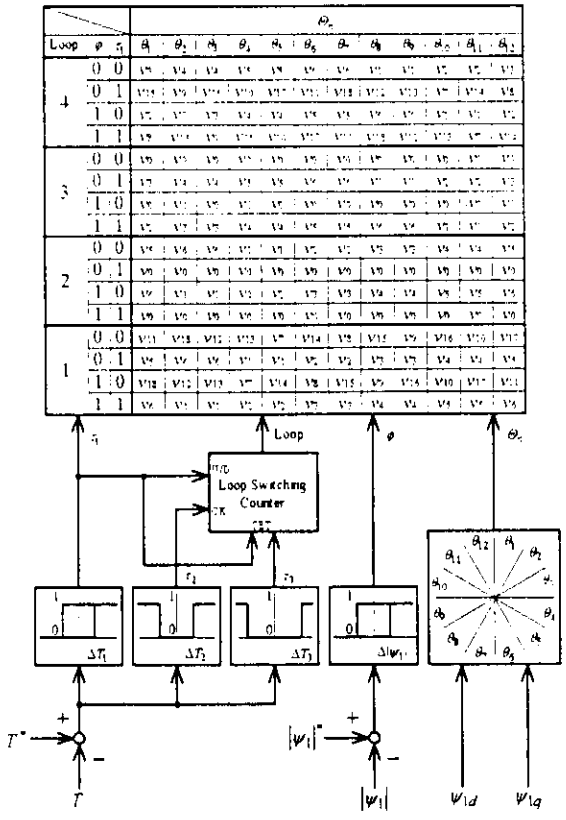

Fig. 5. Flux and torque controller of double parallel PWM inverter.

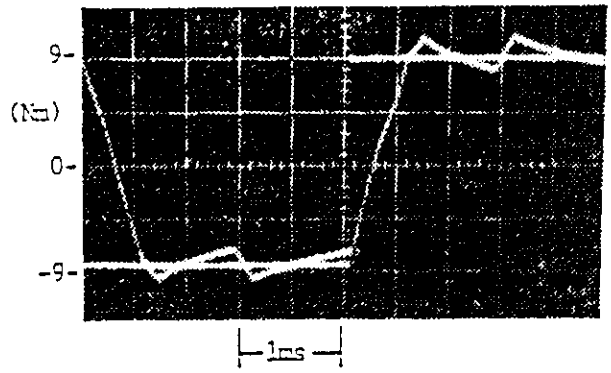

Fig. 6. Step torque response (experimental result).

Fig. 5 shows a schematic diagram of the flux and torque control block which incorporates several hysteresis comparators and a multi-stage switching table. The switching table consists of four sets of the voltage vector selector according to the condition of the output torque level as previously described.

Fig. 6 shows an experimental result of step torque response in time domain. From the figure, it can be seen that the settling time to the rated torque is only 0.6 (ms) and there is neither overshoots nor undershoots in the response. Frequency characteristics for several conditions of the output torque level are shown in Fig. 7. According to the results in frequency domain, although a cut-off frequency varies with the output torque level due to the limit of the inverter output voltage, it is approximately 1 (kHz) for the rated torque.

III. Improvement of Parameter Sensitivity by Advanced On-Line Tuning Technique

It is very important even for the direct torque control to estimate the stator flux with robustness against the motor parameters, especially against the stator and rotor resistance. In this section, a technique which enables to estimate the flux with less sensitivity to the motor parameters is described.

It is well-known that there are two manners to estimate the stator flux with a machine model which includes the motor parameters. One is a stator voltage model, and the other is a rotor current model. The stator voltage model is based on integral calculation of the detected stator voltage vector v_1 and current vector i_1 as follows :

$$\hat{\psi}_1 = \frac{1}{p}\left(v_1 - \hat{R}_1 i_1\right). \qquad (1)$$

where R_1 is the stator resistance. The above model is very

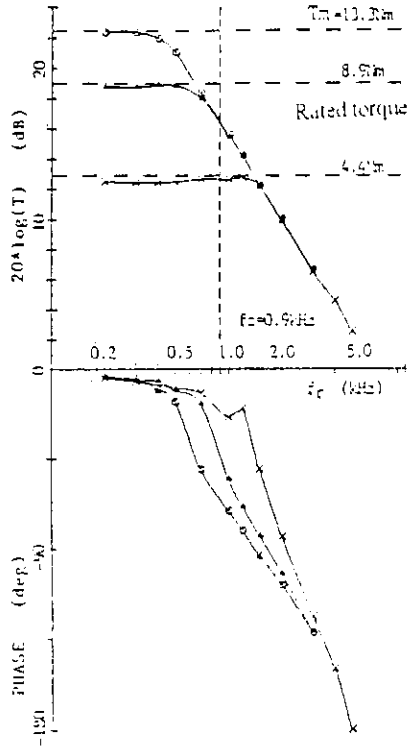

Fig. 7. Frequency responses of torque control (experimental results).

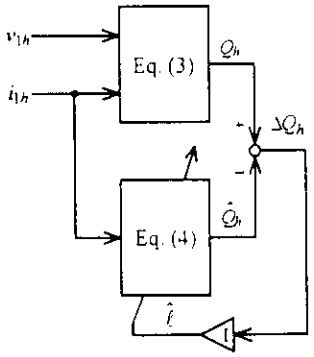

(a) Leakage inductance identifier.

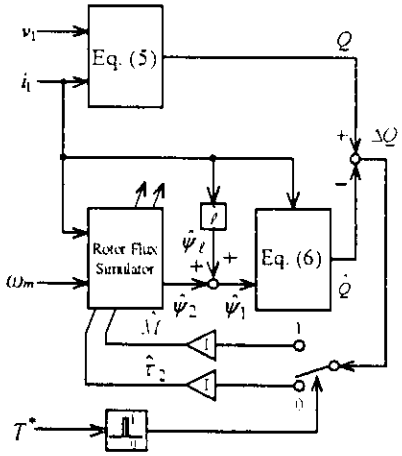

(b) Magnetizing inductance and rotor time constant identifier.

Fig. 8. Robust identifiers of motor parameters.

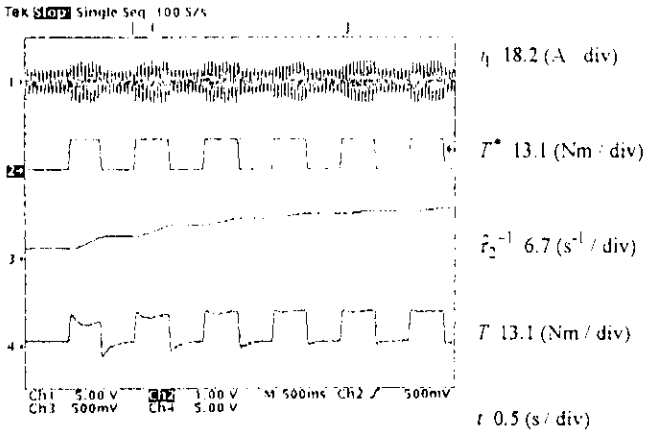

Fig. 9. Parameter identification characteristic (experimental result).

useful because of its simplicity, but can not estimate the $\hat{\psi}_1$ at extremely low speed, especially at zero frequency, because the integration can actually cause errors accumulated in the calculation. On the other hand, the rotor current model can be expressed by the following equation :

$$\hat{\psi}_1 = \hat{\psi}_2 + \hat{\psi}_\ell = \frac{\hat{M}}{1+(p - j\omega_m)\hat{\tau}_2} i_1 + \hat{\ell} i_1 , \qquad (2)$$

where M is magnetizing inductance, τ_2 is rotor time constant and ℓ is leakage inductance. This model requires to detect the rotating speed ω_m, but can estimate the $\hat{\psi}_1$ even at zero frequency because of no pure integrator. However, in order to estimate the $\hat{\psi}_1$ accurately, the on-line identification of the parameters in (2) has to be performed without any sensitivity to the R_1.

Fig. 8 shows schematic diagrams of the parameter identifiers for (2). One of the identifiers is composed for estimation of the ℓ, and the other is for the M and τ_2. When the ℓ is identified, a harmonic voltage vector v_h of which frequency is 500 (Hz) and amplitude is 8 (V) is intentionally injected to the motor. Under this condition, instantaneous harmonic reactive power Q_h is calculated as a reference model according to the following equation :

$$Q_h = \mathrm{Im}\left(v_h \overline{i_h}\right), \qquad (3)$$

where i_h is a harmonic current vector corresponding to the v_h. On the other hand, the estimated value of (3) is calculated to identify the $\hat{\ell}$ as follows :

$$\hat{Q}_h = \hat{\ell}\,\mathrm{Im}\left(p i_h \overline{i_h}\right). \qquad (4)$$

The above equation can be derived from an equivalent circuit of the motor for harmonics. The error between (3) and (4) makes it possible to identify the $\hat{\ell}$ as shown in Fig. 8(a). Since the Q_h has little sensitivity to any other parameters as shown in (3) and (4), it is possible to carry out the robust identification.

When the M and the τ_2 are identified, the instantaneous reactive power Q is utilized in the identifier as shown in Fig. 8(b) detecting fundamental components of the v_1 and the i_1. A true value of the Q can be calculated by

$$Q = \mathrm{Im}\left(v_1 \overline{i_1}\right). \qquad (5)$$

In a similar way, the estimated value of (5) can be obtained by the following equation :

$$\hat{Q} = \mathrm{Im}\left(p\hat{\psi}_1 \overline{i_1}\right). \qquad (6)$$

It should be noted that both (5) and (6) never require the value of the R_1. Therefore, it is possible to identify the $\hat{M}$ and the $\hat{\tau}_2$ by the error between (5) and (6) without any sensitivity to the R_1. In Fig. 8(b), the $\hat{\tau}_2$ is identified at loaded condition, while the $\hat{M}$ is at no load condition.

Fig. 9 shows an example of parameter identification process and step torque response. It can be seen that the torque response is dramatically improved as the identified parameters converge to the true values. Also, it should be noted that this improvement of the torque response can be realized even under the condition of varied R_1 from its nominal value.

IV. Emerging Technology for Further Performance Improvement

Switching frequency of the inverter depends on hysteresis band widths for the stator flux and output torque control, and in principle an acoustically silent motor operation can be done by reducing the hysteresis band widths and using high speed switching devices, for example IGBTs, MOSFETs and so forth. However, the switching frequency of the inverter can not practically be raised even though the band widths are sufficiently reduced because of the delay time in detecting circuits of the stator voltages and currents and in estimating circuits of the flux and torque. Fig. 10 shows the averaged inverter switching frequency against the hysteresis band widths which have been normalized with respect to the rated flux amplitude and the rated output torque per pole pair. If there is no time delay in the feedback signals, the switching frequency is inversely proportional to the hysteresis band width for the flux control as shown in Fig. 10(a). Even in case of only 10 (μs) delay time shown in Fig. 10(b), however, the switching frequency can not be raised although the hysteresis band widths are sufficiently reduced. In order to overcome the

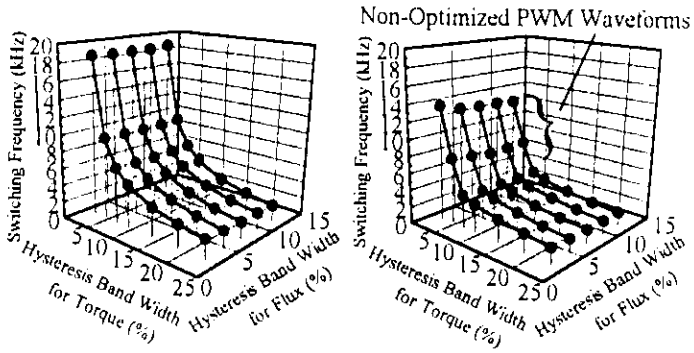

(a) No delay time. (b) 10 (μs) delay time.

Fig. 10. Switching frequency of conventional direct torque control.

problem, dither signals have been introduced into the conventional system, which enable the controller to raise the switching frequency regardless of the delay time.

Fig. 11 shows a schematic diagram of the system. In the figure, triangular waves which are intentionally injected to the flux and torque control blocks correspond to the dither signals. The frequency of the signals is more than 30 (kHz) so that the switching frequency can be approximately 15 (kHz), and their amplitudes are as small as hysteresis band widths for the flux and torque control. Although the hysteresis band inherently acts as a non-sensitive band, the switching operation can be performed in each hysteresis element by superposing the triangular waves even though minute variations of the errors occur.

Fig. 12 shows characteristics of the averaged switching frequency when the dither signals are injected. From the figure, it is known that the switching frequency can be raised more than 15 (kHz) even though there is delay time in the feedback signals. Also, as long as the hysteresis band widths are not so small, the switching frequency can be kept almost constant owing to the dither signals.

Several experimental tests have been conducted under the following four conditions : (a) no dither signal injection, (b) dither signal injection only to the torque error, (c) dither signal injection only to the flux error, and (d) dither signal injection to both errors. Fig. 13 shows the error waveforms for the conditions of (a) and (d). Comparing (d) with (a), both of the flux ripple and the torque ripple are reduced down to 30 (%) when the dither signals are applied to the system. Fig. 14 shows the experimental results of acoustic noise level when the test motor was operated at no load from 100 (rpm) to 1500 (rpm). From the figure, it is clear that the noise level can be reduced to less than 55 (dBA) in case of (d) over the whole speed range.

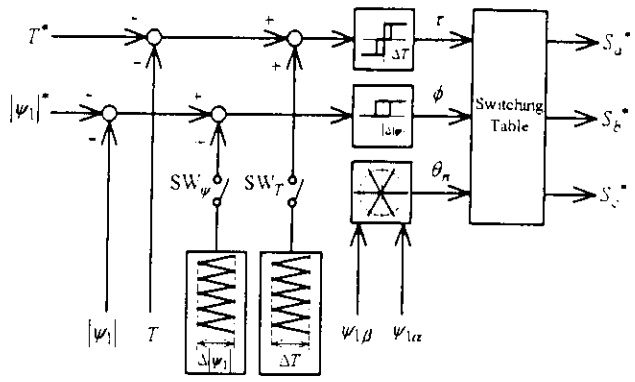

Fig. 11. Direct torque control with dither signal injection.

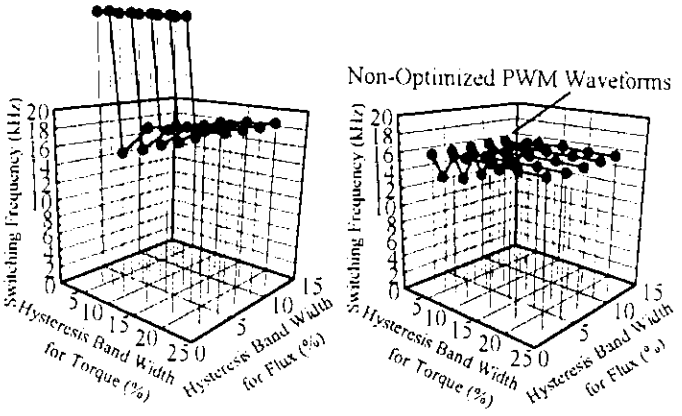

(a) No delay time. (b) 10 (μs) delay time.

Fig. 12. Switching frequency with dither signal injection.

V. Conclusion

The paper has reviewed several key techniques to improve operating characteristics of the direct torque control system. The direct torque control strategy offered a new alternative to obtain a quick torque response with an induction motor, and its basic concept has been established for comprehensive optimization of the motor-inverter system. This aspect is quite different from that of the conventional field-oriented control, because the strategy has been inherently designed assuming compound system of the motor drive fed by the PWM inverter. The direct torque control system fed by a double parallel PWM inverter is one of the solutions to make further improvement of the flux and torque control. The resultant torque response was approximately 1 (kHz), which distinguishes the method from any other control techniques. Furthermore, it should not be forgotten that even the direct torque control has to estimate the stator flux and the output torque, because the system is based on their feedback control. Therefore, the accurate and robust estimation of the feedback

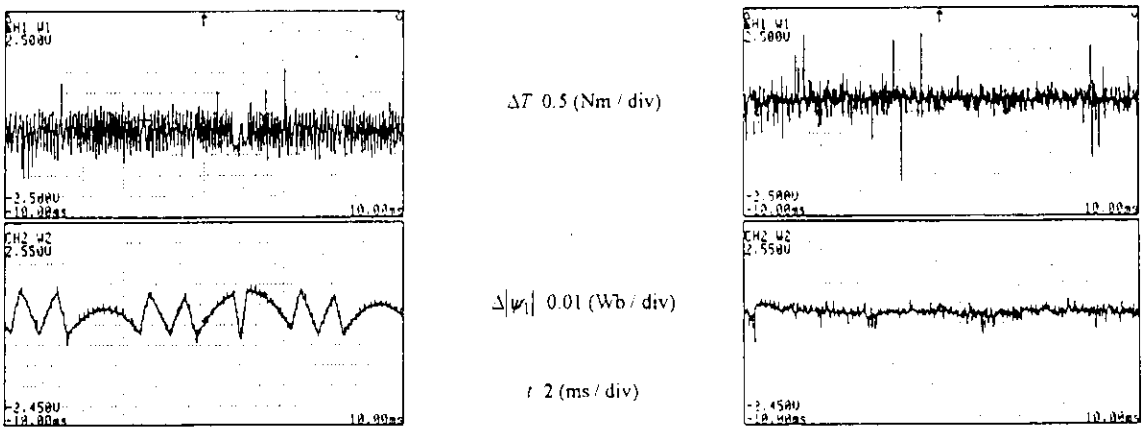

(a) Without dither signal injection. (b) With dither signal injection.

Fig. 13. Stator flux error and torque error waveforms (experimental results).

signals is a substantial problem which can not be avoided. The paper has described an estimation method with robustness against both the stator resistance and the rotor resistance as one of the solutions. Finally, a technique to make the drive acoustically silent has been presented, and it has been shown that the dither signal injection is very effective to reduce the acoustic noise of the motor as well as the ripples of the stator flux and the output torque.

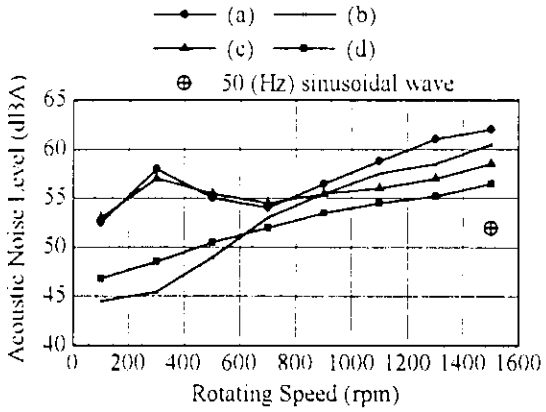

Fig. 14. Acoustic noise level (experimental results).

REFERENCES

[1] Isao Takahashi, and Toshihiko Noguchi, "New quick-Response and High -Efficiency Control Strategy of an Induction Motor," *IEEE IAS Ann. Meet. Conf. Rec.*, pp. 496-502, 1985.

[2] Ichiro Miyashita, Akio Imayanagida, and Isao Takahashi, "High Performance Induction Motor Torque Control Using Digital Signal Processor," *IEE Japan Trans. on Ind. App.*, vol. 107-D, no. 2, pp. 223-230, 1987.

[3] P. Tiitinen, "The Next Generation Motor Control Method, DTC Direct Torque Control," *PEDES - New Delhi Conf. Rec.* , pp. 37-43, 1996.

[4] A. Veltman, "Symmetrical Stator Flux Orbits for Direct Flux and Torque Controlled Drives," *IEEE IAS Ann. Meet. Conf. Rec.*, pp. 197-204, 1996.

[5] Isao Takahashi, and Yoichi Ohmori, "Direct Torque Control of an Induction Motor by a Multi-Parallel PWM Inverter," *IEE Japan Trans. on Ind. App.*, vol. 107-D, no. 10, pp. 1221-1228, 1987.

[6] Toshihiko Noguchi, Seiji Kondo, and Isao Takahashi, "Field-Oriented Control of an Induction Motor with Robust On-Line Tuning of Its Parameters," *IEEE Trans. on Ind. App.*, vol. 33, no. 1, pp. 35-42, 1997.

[7] Toshihiko Noguchi, Masaki Yamamoto, Seiji Kondo, and Isao Takahashi, "High Frequency Switching Operation of PWM Inverter for Direct Torque Control of Induction Motor," *IEEE IAS Ann. Meet. Conf. Rec.*, pp. ???-???, 1997.

APPENDIX

Specifications of the induction motors tested in the simulations and experiments of each section are as follows :

TABLE I SPECIFICATIONS OF TESTED MOTORS

Section of the paper	II	III and IV
Rated Power (kW)	1.5	1.5
Rated Torque (Nm)	10.1	8.64
Rated Voltage (V)	200	180
Rated Current (A)	6.8	8.1
Rated Frequency (Hz)	50	—
Rated Speed (rpm)	1420	1650
Number of Poles	4	4